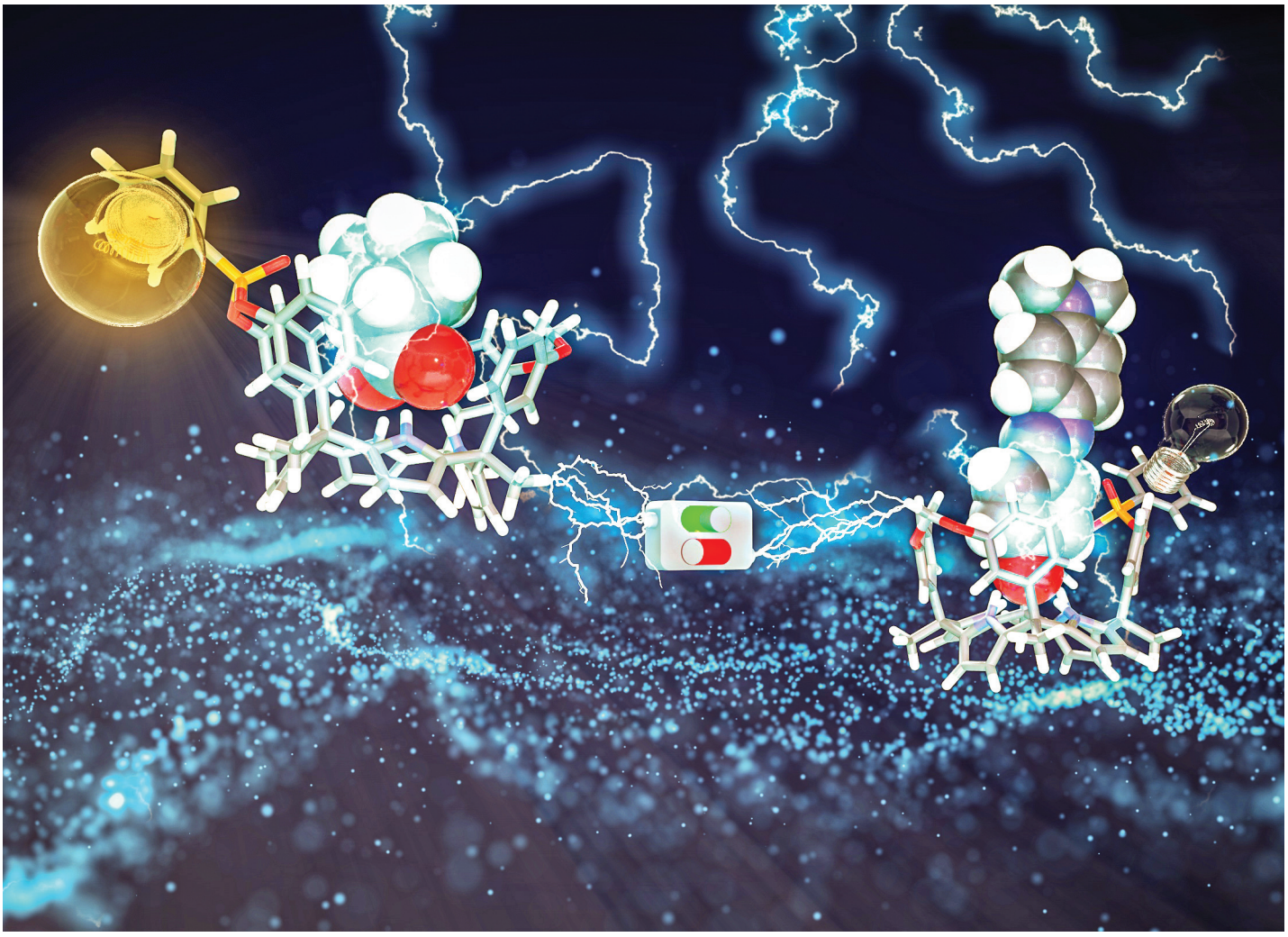

Showcasing research from Professor Ballester's laboratory, School of Chemistry, Institute of Chemical Research of Catalonia (ICIQ), Tarragona, Spain.

Supramolecular fluorescence sensing of L-proline and L-pipecolic acid

We report the synthesis of two diastereomeric mono-phosphonate calix[4]pyrrole cavitands featuring a *N*-phenyl-naphthalamine fluorophore directly attached to its phosphorous atom. The two isomers differ in the relative orientation of the P=O bridging group *in/out* with respect to the polar aromatic cavity. We developed two different supramolecular approaches for the sensing of L-Proline and L-Pipecolic acid using the fluorescent receptors: direct binding-based sensing (BBS) and a FRET-based indicator displacement assay (IDA). Both approaches assigned a binding selectivity for L-Proline to the *in* isomer.

As featured in:

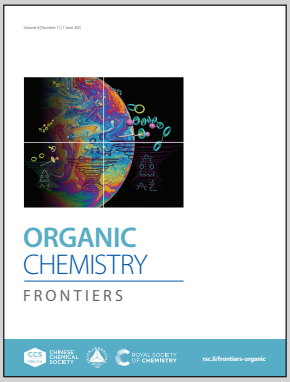

See Pablo Ballester *et al.*, *Org. Chem. Front.*, 2021, **8**, 2402.

CCS 中国化学会 CHINESE CHEMICAL SOCIETY
SIOC 1950
ROYAL SOCIETY OF CHEMISTRY
rsc.li/frontiers-organic

ORGANIC CHEMISTRY FRONTIERS

RESEARCH ARTICLE

View Article Online
View Journal | View Issue

Cite this: *Org. Chem. Front.*, 2021, **8**, 2402

Supramolecular fluorescence sensing of L-proline and L-pipecolic acid†

Andrés Felipe Sierra, [a,b] Gemma Aragay, [a] Guillem Peñuelas-Haro [a] and Pablo Ballester *[a,c]

The current library of synthetic molecular sensors for small polar molecules is limited. In this work, we describe the synthesis of two diastereomeric mono-phosphonate calix[4]pyrrole cavitands, **1in** and **1out**, acting as fluorescent sensors for amino acids. The two isomeric cavitands differ in the relative orientation, *in* (**1in**) and *out* (**1out**), of their P=O bridging group and the *N*-phenyl-naphthalamine fluorophore directly attached to it, with respect to their polar aromatic cavities. Using ^{1}H and ^{31}P NMR spectroscopy and non-fluorescent cavitand analogues (**5in** and **5out**), we demonstrate the formation of 1 : 1 complexes with L-proline (L-Pro) and the relevance of the inwardly directed P=O group in the binding of the amino acid. Only the L-Pro⊂**5in** complex establishes a charged hydrogen bonding interaction between the receptor P=O group and the protonated amine of the bound zwitterionic amino acid. This interaction is responsible for an increase in the thermodynamic stability of the complex compared to the L-Pro⊂**5out** counterpart. We investigate the binding properties of the fluorescent cavitands, **1in** and **1out**, with L-Pro and L-pipecolic acid (L-Pip) at micromolar concentration using emission spectroscopy (direct binding-based sensing, BBS). The observed emission changes in the BBS experiments were small but evidenced the role of the cavitands as fluorescent sensors. In agreement with the millimolar concentration results (^{1}H NMR experiments), the fluorescent **1in** sensor displays a larger binding affinity for L-Pro than the **1out** isomer. Conversely, the **1out** isomer experienced larger emission changes upon amino acid binding. We developed FRET-based indicator displacement assays (IDA) owing to the small emission changes observed in the direct BBS experiments. At micromolar concentration, the competitive displacement of the quencher *N*-oxide **6** from the cavity of the 1 : 1 supramolecular ensemble (**6**⊂**1in** and **6**⊂**1out**), by L-Pro, L-Pip, and L-phenylalanine (L-Phe) produced fluorescence "turn-on". The results of the BBS and IDA experiments assigned a binding selectivity to the **1in** isomer for L-Pro.

Received 7th April 2021,
Accepted 7th April 2021

DOI: 10.1039/d1qo00517k

rsc.li/frontiers-organic

Introduction

There is an increasing demand in monitoring small polar molecules, which are relevant for disease diagnosis and training status, using portable and even wearable sensing devices.[1] Ideally, the developed sensing devices should be designed for direct manipulation by end-users. This characteristic avoids the intervention of trained medical personnel and the commute to point-of-care facilities or hospitals. Moreover, the devices might transmit the results wirelessly to apps installed in mobile phones and share them with the electronic patient's record or the clinician.[2] Biological and synthetic receptors are fundamental components of many small molecule sensing devices related to human health.[3,4] The principle at work is supramolecular sensing, which relies on transduction mechanisms exclusively activated by molecular recognition events.[5,6] This approach offers significant benefits for the design of synthetic selective molecular sensors, as well as for limiting the interferences caused by non-specific binding. Specific binding, *a.k.a* molecular recognition, builds on shape, size and function complementarity between receptor and analyte. In many cases, the transduction mechanism of the binding event demands the covalent incorporation of reporter units to the receptor's scaffolds *i.e.* the fluorescence, absorbance or redox properties of the receptor itself are not suitable for transduction in practical applications. The constructs resulting from the covalent connection of a synthetic receptor to a reporter unit are referred as molecular sensors. Molecular sensors are

[a]*Institute of Chemical Research of Catalonia (ICIQ), The Barcelona Institute of Science and Technology (BIST), Avgda. Països Catalans 16, 43007 Tarragona, Spain. E-mail: pballester@iciq.es*
[b]*Universitat Rovira i Virgili (URV), Departament de Química Analítica i Química Orgànica, c/Marcel·lí Domingo, 1, 43007 Tarragona, Spain.*
[c]*ICREA, Passeig Lluís Companys 23, 08018 Barcelona, Spain*

†Electronic supplementary information (ESI) available: Synthetic procedures, characterization data, UV–Vis and fluorescence titrations, energy minimized structures. CCDC 2053978 and 2053980. For ESI and crystallographic data in CIF or other electronic format see DOI: 10.1039/d1qo00517k

also key in the design of selective sensor nanomaterials able to discriminate analytes by molecular structure (specific binding) rather than by physical/chemical properties *i.e.* polarity (non-specific binding).

Phosphonate calix[4]pyrrole cavitands are synthetic molecular receptors displaying one or more phosphonate bridging groups at the upper rim of "four wall" aryl-extended calix[4]pyrrole scaffolds. In previous studies, we described the use of these receptors for the selective recognition of ion-pairs and small polar neutral molecules.[7,8] We showed that the mono-phosphonate calix[4]pyrrole cavitand **5in** (Fig. 1) provided a three-dimensional polar aromatic cavity suitable for including creatinine and surrounding most of its surface.[9]

The receptor's aromatic cavity is functionalized with an inwardly directed phosphonate group at its open upper rim and by four pyrrole NHs at the opposed and closed end. These polar groups offer complementary hydrogen bonding donor and acceptor interactions to those of the included guest. We used the mono-phosphonate calix[4]pyrrole cavitand scaffold for the construction of ion selective electrodes, molecular sensors and indicator displacement assays for creatinine sensing and quantification.[10,11] More recently, we demonstrated that the mono-phosphonate calix[4]pyrrole cavitand was also an effective synthetic carrier facilitating the selective diffusion of L-proline across membranes of liposomes and living cells.[12] L-Proline is also included in the aromatic cavity of the mono-phosphonate receptors establishing multiple charged hydrogen-bonds (carboxylate-pyrrole NHs, ammonium-phosphonate) and CH–π interactions.

Herein, we describe the synthesis of two novel fluorescent molecular sensors based on a mono-phosphonate calix[4]pyrrole cavitand scaffold. The introduced approach hinges on the covalent attachment of the fluorescent signalling unit directly to the phosphonate bridging group. The design is inspired by the work of Dalcanale and co-workers with mono-phosphonate fluorescent cavitands based on resorcin[4]arene scaffolds.[13] We also report the binding properties of mono-phosphonate calix[4]pyrrole cavitands and their fluorescent derivatives with a reduced series of amino acids: L-proline (L-Pro), L-pipecolic acid (L-Pip) and L-phenylalanine (L-Phe). Using a direct binding-based sensing (BBS) approach, we determined that the binding constant of the fluorescent **1in** isomer for L-Pro was one order of magnitude larger than that of L-Pip. Surprisingly to us, the direct BBS experiments of L-Pro and L-Pip with the **1out** isomer produced larger changes in emission intensity in comparison to those of the **1in** counterpart. Nevertheless, the binding constant values determined for the 1 : 1 inclusion complexes of **1out** and the amino acids were one order of magnitude smaller than those of the **1in** isomer. Due to the small changes observed with the direct BBS approach, we considered that an improved fluorescent sensing of the amino acids required the development of indicator displacement assays (IDA).[14] To this end, we used the pyridine-*N*-oxide **6** as analogue of the well-known DABCYL ((4-dimethylaminoazo)benzene-4-carboxylic acid) black-hole quencher (Fig. 1). Pyridine *N*-oxide **6** formed thermodynamically and kinetically highly stable 1 : 1 non-emissive complexes with **1in** and **1out**. The displacement of **6** from the 1 : 1 complexes produced fluorescence "turn-on". The BBS and IDA experiments produced analogous binding constant values for all complexes. They assigned a superior stability to the L-Pro⊂**1in** complex compared to L-Pip⊂**1in** and L-Phe⊂**1in** analogues, and the **1out** counterparts. The obtained binding results are supported by direct inspection of the molecular interactions present in the energy-minimized structures of the inclusion complexes.

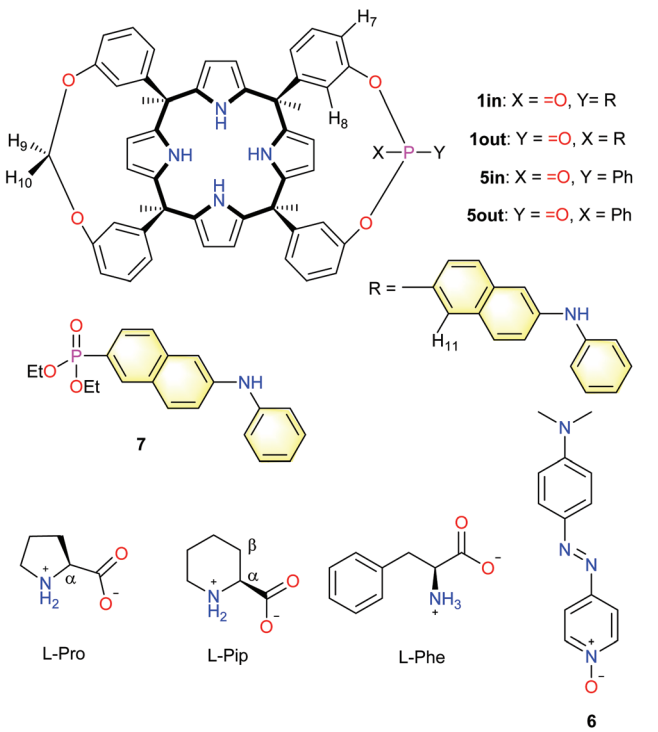

Fig. 1 Line drawing molecular structures of the monophosphonate calix[4]pyrrole cavitands **1in**/**1out** and **5in**/**5out**, the pyridine *N*-oxide quencher **6**, diethyl 6-(phenylamino)naphthalene-2-phosphonate **7** and the substrates used in the work (L-Pro, L-Pip and L-Phe). Proton assignment of calix[4]pyrrole cavitands and amino acids is shown in the structure.

Results and discussion

Synthesis

The fluorescent phosphonate calix[4]pyrrole cavitands **1in** and **1out** were prepared in two synthetic steps starting from the known α,α,α,α-isomer of tetra-*meta*-hydroxyphenyl-tetramethyl-calix[4]pyrrole **2** (Scheme 1).[7] Firstly, the mono-methylene bridged calix[4]pyrrole **3** was obtained by reacting α,α,α,α-**2** tetrol with 1.2 equiv. of bromochloromethane in DMSO solution in the presence of potassium carbonate as base. The mono-methylene bridged compound **3** was isolated in 48% yield after column chromatography purification of the reaction

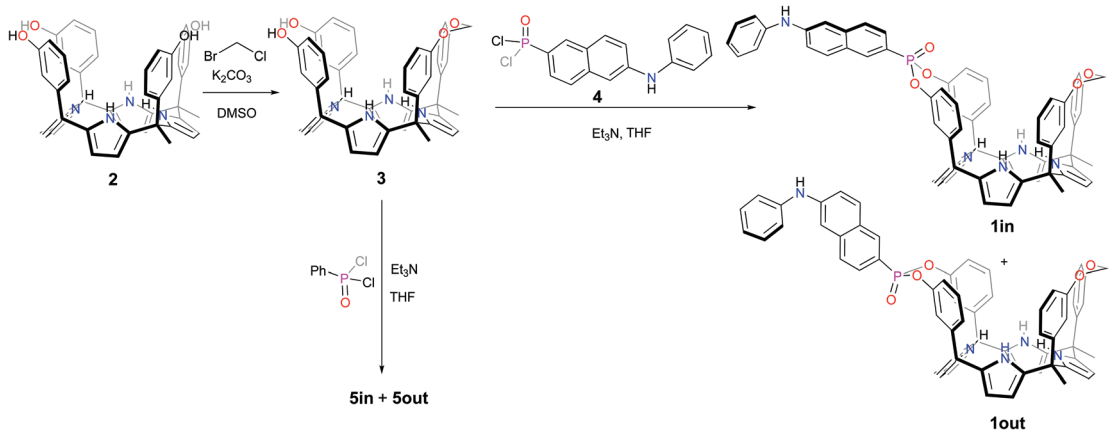

Scheme 1 Synthetic scheme for the preparation of the isomeric mono-phosphonate mono-methylene fluorescent calix[4]pyrrole cavitands **1in** and **1out** and non-fluorescent analogues **5in** and **5out**.

crude and crystallization of the isolated fraction in acetonitrile. Secondly, the incorporation of the fluorescent unit at the upper rim of **3** involved the room temperature reaction with freshly prepared 6-(phenylamino)-naphthalen-2-yl phosphonic acid dichloride **4**,[13] in THF solution during 2h and using triethylamine as base. The reaction produced a mixture of the two mono-phosphonate diastereoisomers **1in** and **1out**. The two pure stereoisomers were isolated by separation of an enriched fraction of the reaction crude (see ESI† for details) by means of analytical HPLC (Waters Spherisorb®, 5.0 μm Silica, 4.6 mm × 250 mm) using isocratic elution (DCM : AcOEt 90 : 10).

The **1out** isomer eluted first. The **1in** isomer, presenting the P═O group inwardly oriented with respect to its aromatic cavity, was more polar and eluted second. This latter arrangement of functional groups should allow that suitable bound guests can establish simultaneous hydrogen-bonding intermolecular interactions with both the P═O group and the NHs of the calix[4]pyrrole core of the fluorescent receptor. The isolated **1out** isomer will be used as a control to validate this hypothesis.

The configurational assignment of the two diastereoisomeric cavitands, **1in** and **1out**, was achieved by a combination of ^{1}H, ^{31}P NMR spectroscopy and X-ray crystallographic analysis. Single crystals of **1in** grew from a deuterated acetone solution used to acquire its NMR spectra. On the other hand, we used acetonitrile to obtain single crystals of **1out**. The solid-state structures of the two fluorescent calix[4]pyrrole isomers are depicted in Fig. 2. In both of them, the calix[4]pyrrole core adopts the cone conformation and one molecule of the solvent, used to grow the crystals, is included in its polar aromatic cavity. The included solvent forms four simultaneous hydrogen-bonding interactions between its heteroatom (oxygen or nitrogen) and the pyrrole NHs. In the solid state and for the two isomers, the 14-membered rings delineated by the bridged phosphonate-group, two *meso*-phenyl groups, their corresponding *meso*-carbons and one

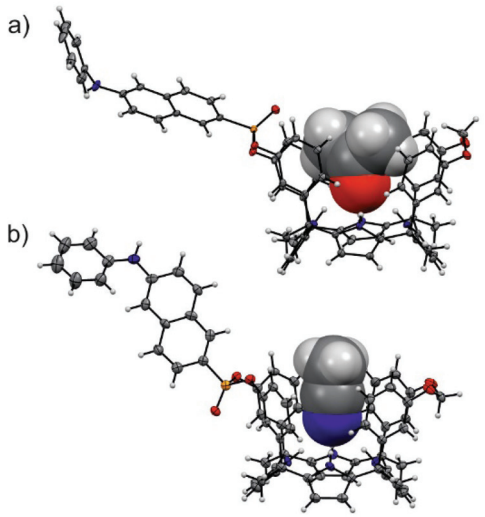

Fig. 2 Solid-state structures of the two diastereoisomeric fluorescent receptors, **1in** (a) and **1out** (b). The structures of the receptors are shown in ORTEP view with thermal ellipsoids set at 50% probability. Hydrogens are shown as fixed-size spheres of 0.3 Å radius. The included solvent molecules (acetone and acetonitrile) are displayed as space-filling models.

pyrrole ring, present a conformation locating the phenylamino-naphthyl substituent of the phosphorous atom in equatorial orientation and pointing away from the aromatic cavity.

The outwardly oriented fluorescent unit, which is observed in both solid-state structures of the calix[4]pyrrole diastereoisomers, is in striking contrast to the observation made in structurally related isomers of mono-phosphonate resorcin[4]arene cavitands.[13] In the latter case, the ^{1}H NMR spectrum of the *out* isomer showed the protons assigned to the phenylamino-naphthyl substituent upfield shifted compared to those of the *in* counterpart. This difference was attributed to dissimi-

lar orientations of the substituent with respect to the receptor's aromatic cavity. In short, the resorcin[4]arene *out* isomer directs the fluorescent substituent towards the receptor's cavity experiencing the shielding effect exerted by the aromatic rings.

We did not observe significant chemical shift changes for the signals of the hydrogen atoms of the fluorescent substituent when comparing the ^{1}H NMR spectra of the **1in** and **1out** isomers in acetone-d_6 or dichloromethane-d_2 solutions (Fig. 3). This finding indicated that in agreement with the solid-state structures, in solution, the two isomers of **1** also featured the fluorescent substituent outwardly directed with respect to their aromatic cavities. However, the signals for H_8 and H_7 (Fig. 1), corresponding to the *meso*-aryl hydrogen atoms that are *ortho* with respect to the bridging phosphonate group, showed very different chemical shift values in the two isomers. For example, in the **1out** isomer H_8 resonates significantly downfield shifted compared to the chemical shift value for the analogous proton signal in the **1in** counterpart (Fig. 3). This chemical shift difference is due to the positioning of H_8 in the deshielding zone of the magnetic anisotropy cone generated by the *out* P═O group. For the same token, proton H_7 becomes partially deshielded when the P═O group is inwardly directed.

The chemical shift values of the phosphorous atoms of the **1in** and **1out** isomers are in agreement with those observed for structurally related mono- and bis-phosphonate calix[4]pyrrole cavitands (Fig. S12 and S20†).[7,9] The phosphorous atom of the out isomer resonates slightly upfield, possibly due to the shielding effect exerted by the aromatic cavity. In acetone-d_6 solution, both isomers showed three highly downfield shifted signals for the pyrrole NHs. This is due to the involvement of the NHs in hydrogen bonding interactions with the oxygen atom of one included acetone molecule. The bound acetone molecule locks the cavitands in their cone conformation as observed for **1in** in the solid-state (Fig. 2a). The ^{1}H NMR spectra of the two isomers in chlorinated solvents (*vide infra*) are significantly different to those registered in acetone. Most likely, in dichloromethane-d_2 solution the receptors adopted alternate conformations of their calix[4]pyrrole core and are involved in conformation exchange processes that are fast on the chemical shift timescale.

NMR binding studies

We became interested in investigating the binding properties of these type of cavitands as receptors for L-Pro and the 6-membered ring α-amino acid analogue, L-pipecolic acid (L-Pip). L-Pip has been described as a diagnostic marker of pyridoxine-dependent epilepsy.[15]

We first performed separate solid–liquid extraction experiments with L-Pro or L-Pip and the fluorescent cavitand **1in** in CD_2Cl_2. We added an excess of the solid amino acid (~2mg L-Pro or L-Pip) to a 2 mM CD_2Cl_2 solution of the cavitand **1in**. We hand-shook the suspensions for several minutes and filtered off the remaining solid. The ^{1}H NMR spectra of the filtered solutions showed significant differences compared to that of the free cavitand **1in** in the same solvent (Fig. 4). In both cases, only a single set of sharp signals was observed for the hydrogen atoms of the receptor.

The signals corresponding to the pyrrole NHs were the ones experiencing the most important chemical shift changes. These signals moved downfield compared to those in free **1in** ($\Delta\delta$ = 1.8–1.5 and 2.3–1.1 ppm, for L-Pro and L-Pip, respectively), suggesting their involvement in hydrogen bonding interactions with the corresponding included guest. On the other hand, we observed the appearance of a new set of signals in the upfield region of the spectra. These signals were indicative of the inclusion of the guests in the polar aromatic cavity of **1in**. Specifically for L-Pro extraction, we observed a broad signal centred at δ = 2.7 ppm. We attributed this signal to the proton α to the carboxylate group of the bound L-Pro. This signal appeared upfield shifted compared to that of the free guest in $(CD_3)_2SO$ solution ($\Delta\delta$ = −1.2 ppm). Thus, the proton atoms of the included L-Pro experienced the shielding effect exerted by the four *meso*-phenyl substituents of **1in**. Analogously, the signals of bound L-Pip also appeared upfield

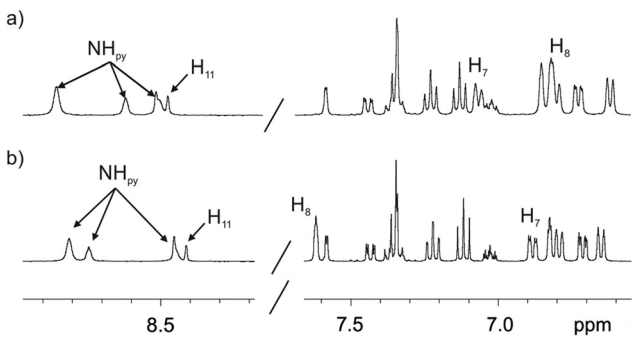

Fig. 3 Selected regions of the ^{1}H (400 MHz, 298 K) spectra of **1in** (a) and **1out** (b) isomers in acetone-d_6 solution. The pyrrole NH, β-pyrrole, H_{11} and the two proton signals of the *meso*-aryl groups, H_8 and H_7, that are *ortho* with respect to the phosphonate bridging groups are indicated. See Fig. 1 for proton assignment.

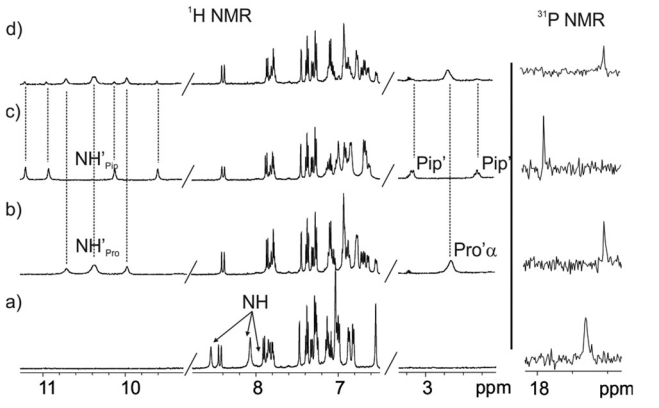

Fig. 4 ^{1}H NMR (400 MHz, 298 K) and ^{31}P NMR spectra of a 2 mM CD_2Cl_2 solution of **1in** before (a) and after (b–d) solid–liquid extraction with solid L-Pro (b) and solid L-Pip (c) and with equal amounts of solid L-Pro and L-Pip (d).

shifted compared to those in the free guest in $(CD_3)_2SO$ solution. The integral values of selected proton signals for the host and the guest indicated the quantitative formation of 1 : 1 complexes: L-Pro⊂**1in** and L-Pip⊂**1in**. That is, receptor **1in** extracted 1 equiv. of L-Pro and L-Pip in the independent solid–liquid extractions experiments.

The binding of the guest was also supported by the chemical shift changes observed in the ^{31}P NMR spectra of the filtered solutions. The ^{31}P NMR spectrum of free **1in** shows a singlet resonating at δ = 17.3 ppm. Remarkably, after the extraction experiments of L-Pro and L-Pip, the phosphorous signal of bound **1in** resonated at δ = 17.0 ppm and 17.9 ppm, respectively (Fig. 4 right).

Next, we performed a competitive solid–liquid extraction experiment by adding equimolar amounts of solid L-Pro and L-Pip (~2 mg of each guest) to a millimolar CD_2Cl_2 solution of the fluorescent receptor **1in**. The ^1H NMR spectra of the filtered solution clearly showed two sets of proton signals for the NHs of bound **1in**. Moreover, the integral values of the two sets of NH signals were significantly different (Fig. 4d). By comparison to the ^1H NMR spectra of the solid–liquid extraction experiments performed separately, we easily assigned the two sets of signals to the protons of the bound receptor in the L-Pro⊂**1in** and L-Pip⊂**1in** complexes (Fig. 4b and c). Integration of the pyrrole NH signals for the two complexes assigned a 5 : 1 molar ratio to the mixture of L-Pro⊂**1in** and L-Pip⊂**1in** complexes.‡ Considering that the solubility of L-Pro is slightly higher than that of L-Pip, the result of the competitive extraction experiment is not conclusive in assigning a larger binding affinity of **1in** for L-Pro compared to L-Pip.§ Nevertheless, it provides an initial hint in this direction.

We were also interested in evaluating the importance of the hydrogen bonding interaction established between the inwardly directed P═O group of cavitand **1in** and the protonated amino group of the bound amino acid guests. With this aim, we performed analogous solid–liquid extraction experiments of L-Pro with non-fluorescent cavitands **5in** and **5out**. We used the non-fluorescent receptors as model compounds of the fluorescent counterparts due to their ease of synthesis (Fig. 1). We hypothesized that **5out** could bind and extract L-Pro through the formation of four hydrogen bonds with the pyrrole NHs and additional CH–π interactions. In contrast, the outwardly directed P═O group of **5out** should not participate in hydrogen bonding interactions with the protonated amino group of bound L-Pro. Thus, we expected a decrease in the binding constant of the L-Pro⊂**5out** complex compared to that of the **5in** isomer.

The solid–liquid extraction experiments of L-Pro using the non-fluorescent model receptor **5in** produced similar changes in the ^1H and ^{31}P NMR spectra to those described above for the fluorescent cavitand **1in** (Fig. 4). To our surprise, the ^1H NMR spectrum of the filtered solution obtained after extraction of L-Pro with **5out** showed broad proton signals. The corresponding ^{31}P NMR spectrum did not produce any observable signal. We detected a significant increase in the signal-to-noise ratio of the spectra. We considered this observation as indicative of a diminution of the concentration of **5out** in solution after the extraction experiment. To clarify this issue, we evaporated the CD_2Cl_2 and re-dissolved the solid residue in $(CD_3)_2SO$. The obtained $(CD_3)_2SO$ solution was analysed using ^1H NMR spectroscopy. We observed the diagnostic signals of the protons of free **5out** and free L-Pro. The L-Pro signals displayed a significantly reduced intensity. This result suggested that **5out** was not able to extract 1 equiv. of L-Pro. To investigate the insolubility of the putatively formed L-Pro⊂**5out** complex in CD_2Cl_2, we acquired a ^1H NMR spectrum of the filtered solid by dissolving it in $(CD_3)_2SO$. The ^1H NMR spectrum of the solution displayed the diagnostic signals of free **5out** and free L-Pro. The observation of the signals of free **5out** indicates that the L-Pro⊂**5out** complex features a reduced solubility in CD_2Cl_2, falling out of solution during the solid–liquid experiment and hampering its use for quantitative purposes.

For this reason, we decided to perform a competitive binding experiment starting from a millimolar CD_2Cl_2 solution of the L-Pro⊂**5in** complex. The addition of 1 equiv. of the **5out** isomer to the above solution did not induce significant changes to the proton signals of the L-Pro⊂**5in** complex (Fig. 5b). We detected the appearance of a new set of proton signals that almost coincided with those of the free **5out** receptor. The broadening and small chemical shift changes observed for the new set of signals (Fig. 5b) suggested the existence of a binding equilibrium in solution. In short, we propose that the L-Pro⊂**5out** complex is formed in solution to a reduced extent and the binding equilibrium between free and bound **5out** shows fast/intermediate exchange dynamics on the chemical shift timescale. The ^{31}P NMR spectrum of the mixture also supports this hypothesis. It displayed two singlets centred at δ = 15.8 and 13.4 ppm. The one appearing downfield is quite sharp and corresponds to the L-Pro⊂**5in** complex.

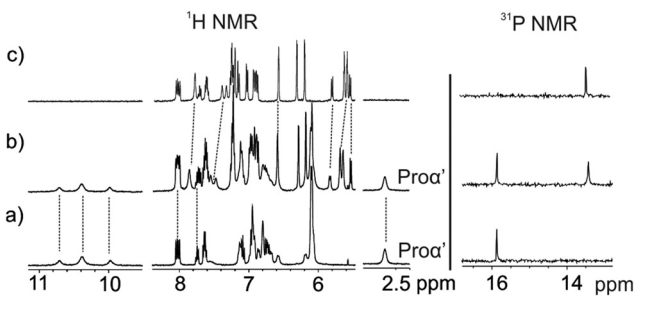

Fig. 5 ^1H NMR (400 MHz, 298 K) and ^{31}P NMR spectra of a CD_2Cl_2 solution of L-Pro⊂**5in** complex before (a) and after (b) the addition of 1 equiv. of **5out**. (c) ^1H and ^{31}P NMR of a CD_2Cl_2 solution of **5out**.

‡We performed an additional solid–liquid extraction competitive experiment in which we left the suspension under stirring overnight. The ^1H NMR spectra of the filtered solution did not show significant changes to the one obtained after 5 minutes hand-shook extraction.

§Solubility was calculated by preparing 1 mL saturated solutions of L-Pro and L-Pip in dichloromethane at 298 K. Evaporation of the solvent and accurate weight of the resulting solids returned the solubility of L-Pro and L-Pip in dichloromethane as 8×10^{-4} and 5×10^{-4} mol L^{-1}, respectively.

In contrast, the upfield-shifted singlet is slightly broadened due to the chemical exchange between free and bound **5out**. The lack of separate signals for the phosphorous atoms of free **5in** results from its low concentration in solution (Fig. 5b, right). Taken together, these results indicate that the binding affinity of **5in** for L-Pro is significantly larger (approximately 7–10-fold, *vide infra*) than that of the **5out** isomer. We attributed the increased binding affinity to the additional hydrogen bond interaction provided by the inwardly directed P═O group in the L-Pro⊂**5in** complex.

UV–Vis and emission spectroscopy binding studies

Direct binding-based sensing (BBS). After having demonstrated the important contribution of the inwardly directed P═O group for the binding of L-Pro with the **5in** model cavitand, we carried out direct binding-based sensing (BBS) studies with the analogous fluorescent **1in** cavitand. Some years ago, Dalcanale and co-workers reported the use of somewhat structurally related fluorescent resorcin[4]arene receptors for the optical sensing of alkyl-chain C_1–C_4 alcohols.[13] The authors claimed that the hydrogen bonding interaction established between the alcohol OH function and the P═O group of the receptor could decrease the electronic density on the phosphorus atom and modify the energy of the excited state of the naphthalene unit directly attached to it. The electronic modification was expected to alter the maximum of the emission band.

The UV–Vis absorption spectra of **1in** and **1out** showed very similar features (Fig. S21†). Concretely, two intense absorption bands with maxima at 275 (ε = 34 000 M^{-1} cm^{-1}) and 328 nm (ε = 24 000 M^{-1} cm^{-1}) and a shoulder at 370 nm. These bands are characteristic of π–π* and n–π*-transitions of the phenylamino-naphthyl moiety, as demonstrated by simple comparison with the UV–Vis spectrum of diethyl 6-(phenylamino) naphthalene-2-phosphonate **7** (Fig. 1) used as model compound (Fig. S22†).

The incremental addition of L-Pro to separate micromolar dichloromethane solutions of **1in** and **1out** did not produce changes in their corresponding UV–Vis spectra (Fig. S24†). Spectral changes were more evident using emission spectroscopy to monitor the titration experiment. The excitation at 335 nm of a 5 × 10^{-7} M dichloromethane solution of **1in** resulted in an intense and broad emission band with a maximum at 422 nm. The incremental addition of L-Pro provoked a concomitant red-shift of the maximum ($\Delta\lambda_{max}$ = 3–4 nm) and a decrease in emission intensity (Fig. 6a). Similar changes were observed during the incremental addition of L-Pip to **1in** using analogous experimental conditions (Fig. S26†).

We also performed emission titration experiments with the fluorescent compound **7**. This compound was used as reference of the fluorescent signalling unit incorporated in the **1in** and **1out** receptor cavitands. In this case, the incremental addition of L-Pro did not produce noticeable changes in the emission of **7** (Fig. S23†). This result evidenced the relevance of the aryl-extended calix[4]pyrrole scaffold for the efficient binding of L-Pro by **1in** and the transduction of the binding event in the modification of the emission properties of the signalling unit.

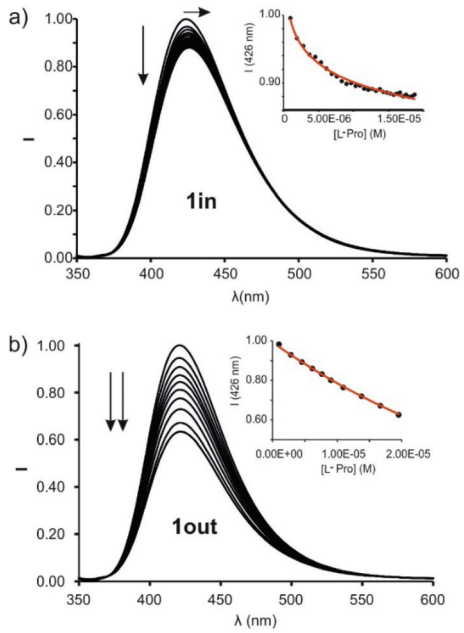

Fig. 6 Normalized emission spectra of **1in** (a) (0.5 μM) and **1out** (1 μM) (b) registered during the addition of incremental amounts of L-Pro (up to 30 equiv. and 20 equiv., respectively) in dichloromethane solution: λ_{exc} = 335 nm. Insets: Plot of the emission change at 426 nm (black circles) *vs.* concentration of L-Pro. The red line corresponds to the fit of the titration data to a 1 : 1 binding model considering two emissive species: the free cavitand and the 1 : 1 complex with the corresponding amino acid.

The changes in emission intensity observed during the titrations of **1in** with L-Pro and L-Pip were rather small. Even so, we fit the obtained experimental titration data to a theoretical 1 : 1 binding model considering two emissive species: free and bound **1in**. We determined the binding constant values for the complexes of **1in** with L-Pro and L-Pip as, K(L-Pro⊂**1in**)$_{BBS}$ = 3.2 × 10^5 M^{-1} and K(L-Pip⊂**1in**)$_{BBS}$ = 6.3 × 10^4 M^{-1}, respectively. Surprisingly to us, the titrations of the **1out** isomer with L-Pro and L-Pip produced greater emission intensity changes (Fig. 6b and S27†).¶ Conversely, the bathochromic shift experienced by the emission band of **1out** was reduced compared to that of **1in** ($\Delta\lambda_{max}$ < 1 nm). The mathematical analysis of the titration data of **1out**, using a 1 : 1 binding model considering two emissive species, returned very similar binding constant values for the two complexes of the amino-acids, K(L-Pro⊂**1out**)$_{BBS}$ = 3.9 × 10^4 M^{-1} and K(L-Pip⊂**1out**)$_{BBS}$ = 2.3 × 10^4 M^{-1}. The magnitudes of the binding constants for the complexes with **1out** are close to one order of magnitude lower than those of the **1in** isomer.

The observation of larger emission changes in the titrations of the **1out** isomer was completely unexpected. The spatial

¶We did not find significant differences in the fluorescence emission of **1in** and **1out** in dichloromethane.

orientation of the P═O group in the free isomer and its complexes is not geometrically suitable for the involvement in charged hydrogen bonding interactions with the bound guests. Dalcanale *et al.* hypothesized that hydrogen bonding interactions with the inwardly directed P═O group were responsible for the observed emission changes in the gas-phase sensing of short alkyl chain alcohols using structurally related phosphonate resorcin[4]arene cavitands. The authors did not observe emission changes in the sensing experiments using the out isomer. Based on our findings, we suggest that the cavitand-amino acid binding, especially for the **1out** isomer, induces changes in the conformation (and possibly steric effects) of the receptor, which directly affects the properties of the signalling unit. These changes are transduced into non-radiative decay processes of the excited states of the 1 : 1 complexes. Accordingly, the binding event is responsible for the observed decrease in fluorescence intensity of the signaling unit.‖

Development of an Indicator Displacement Assay (IDA): a study of the interaction of the fluorescent receptors 1in and 1out with N-oxide 6. The reduced changes observed in the direct BBS fluorescence titrations of **1in** with the two amino acids prompted us to explore an alternative sensing approach using an Indicator Displacement Assay (IDA). Recently, we described the synthesis and characterization of the pyridyl-*N*-oxide derivative **6** (Fig. 1). The molecular structure of **6** is based on the popular and efficient acceptor 4-(dimethylaminoazo)benzene-4-carboxylic acid (DABCYL) ($\lambda_{abs,max}$ = 480 nm, ε = 39 500 M^{-1} cm^{-1}). DABCYL is used in the development of Förster resonance energy transfer (FRET)-based nucleic acid probes. We already applied *N*-oxide **6** for the optical sensing of creatinine using an IDA. We used a calix[4]pyrrole phosphonate cavitand equipped with a dansyl group as fluorophore. We reported that the binding of **6** in the cavity of the receptor produced the efficient quenching of the fluorescence of the dansyl group through a FRET process.[11]

We calculated the spectral overlap between the absorption spectrum of *N*-oxide **6** and the emission spectrum of **1in** to be $J = 2.5 \times 10^{-9}$ cm^6 mol^{-1} (Fig. S28†). This value is even larger than the one calculated for the FRET pair formed by **6** and the phosphonate calix[4]pyrrole containing the dansyl fluorophore, which resulted in *ca.* 95% quenching of the receptor's fluorescence in the 1 : 1 complex. The addition of 1 equiv. of **6** to a 5 μM dichloromethane solution of **1in** produced a strong quenching of the emission band of the receptor at 422 nm (>95%, λ_{exc} = 335 nm) (Fig. S30†).** The fluorescence quenching is the direct consequence of the FRET process operating in the formed 1 : 1 inclusion complex. The phenyl-amino-

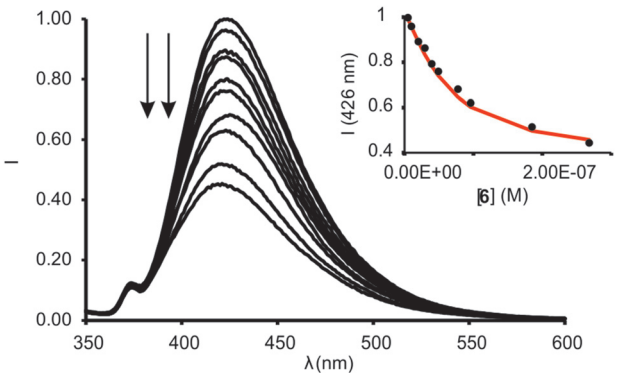

Fig. 7 Normalized emission spectra registered for the titration of **1in** (0.05 μM) with incremental amounts of **6** (up to 4 equiv.) in dichloromethane solution: λ_{exc} = 335 nm. Inset: plot of the emission change at 426 nm (black circles) vs concentration of **6**. The red line corresponds to the fit of the titration data to a 1 : 1 binding model considering two emissive species: free receptor and 1 : 1 complex with **6**.

naphthyl substituent of the **1in** receptor acts as energy donor and the bound ***N*-oxide 6** as the acceptor. We obtained analogous results for the equimolar mixture of **1out** and **6** (Fig. S31†). The quantitative formation of the complexes **6⊂1in** and **6⊂1out** in the presence of 1 equiv. of the *N*-oxide allowed us to estimate their binding constants as larger than 10^7 M^{-1}. We expected similar binding constant values for the two complexes owing to the lack of additional interaction of guest **6** with the P═O group of the receptors. We performed a titration of **1in** with **6** using more diluted conditions ([**1in**] = 5×10^{-8} M, Fig. 7) and determined the accurate binding constant of the 1 : 1 complex to be K(**6⊂1in**) = 3.2×10^7 M^{-1}.†† The incremental addition of **6** to a 1μM solution of **7**, used as reference of the fluorescent substituent of the receptors, did not produce noticeable emission changes. This result demonstrated that the formation of the 1 : 1 complexes induces the observation of the FRET-quenching process.

Competitive IDA experiments. Initially, we probed the competitive binding of **6** and L-Pro with the **1in** receptor using ^{1}H NMR spectroscopy. We prepared an equimolar CD_2Cl_2 solution of **1in** and L-Pro ([**1in**] = [L-Pro] = 2.0 mM) by performing a solid–liquid extraction experiment (Fig. 8a). The ^{1}H NMR spectrum of the obtained solution revealed the exclusive presence of the diagnostic signals for the quantitative formation of the L-Pro**⊂1in** complex. The subsequent addition of 0.5 equiv. of **6** produced the appearance of a separate set of signals (Fig. 8b). We attributed the new set of signals to the protons of the receptor in the **6⊂1in** complex. The observation of two separate sets of signals for the receptor's protons in the L-Pro**⊂1in** and

‖We did not see the formation of any precipitate after the addition of L-Pip to a micromolar dichloromethane solution of **1out** as observed in the analogous experiments at millimolar concentration (*i.e.* NMR experiments). We consider that at micromolar concentration the L-Pip**⊂1out** complex is soluble in dichloromethane. Therefore, we conclude that the decrease in fluorescence intensity is not related to the precipitation of the complex.

**Slit width of the monochromator as 1 nm.

††These experimental conditions forced us to modify the slit width of the monochromator settings (from 1 nm to 5 nm). These new parameters did not allow us to consider the **6⊂1in** host–guest complex non-emissive as occurred with the previous instrument set-up. Hence, the titration data was fit to a theoretical 1 : 1 binding model that considered two emissive species (free and bound **1in**).

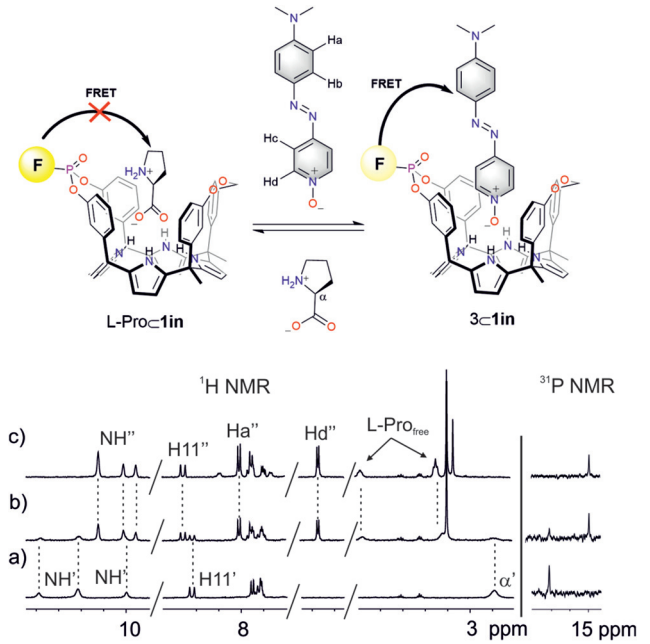

Fig. 8 (Top) Competitive IDA binding equilibrium. (Bottom) ^{1}H and ^{31}P NMR spectra of a 2 mM solution of L-Pro⊂**1in** in CD_2Cl_2 after the addition of 0 (a), 0.5 (b) and 1.0 (c) equiv. of **6**. F denotes the fluorophore: phenyl-amino-naphthyl group.

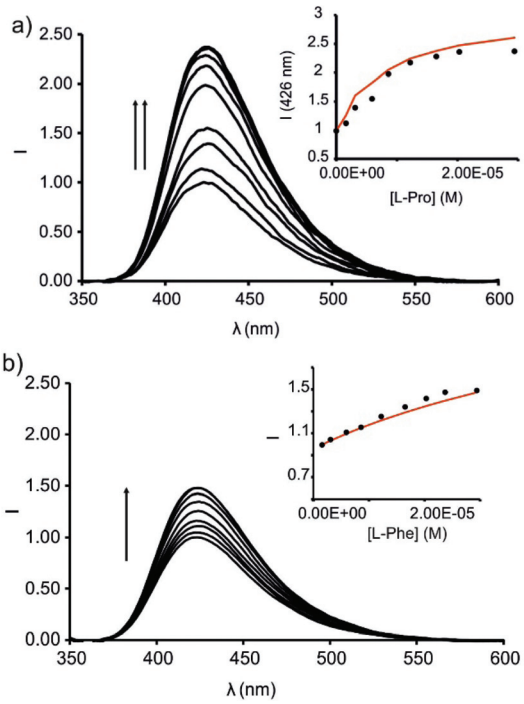

Fig. 9 Emission spectra registered during the competitive IDA experiments of **6**⊂**1in** complex (1 μM) with incremental addition of L-Pro (up to 30 equiv.) (a) and L-Phe (up to 30 equiv.) (b) in dichloromethane solution; λ_{exc} = 335 nm. Insets: plots of the emission change at 426 nm (black circles) *vs*. concentration of the amino acid. The red line corresponds to the fit of the titration data to a 1 : 1 theoretical binding model considering only two emissive species: the free cavitand and the 1 : 1 complex with the corresponding amino acid.

6⊂**1in** complexes indicated that its chemical exchange is slow on the chemical shift timescale. The protons of the pyridyl-*N*-oxide residue of **6** were shifted upfield, in comparison to the free counterpart, placing them within the aromatic walls of the cavitand. Compound **6** is included in the cavity of **1in** by establishing four hydrogen bonds between the oxygen atom of the pyridyl-*N*-oxide knob and the four pyrrole NHs of the receptor in addition to π–π and CH–π interactions. We also observed a new set of signals in the downfield region of the spectrum and we assigned them to the protons of free L-Pro. The addition of 1 equiv. of **6** induced the exclusive observation of the proton signals of the receptor in the **6**⊂**1in** complex. Concomitantly, the signals of free L-Pro grew in intensity (Fig. 8c). This result is in complete agreement with the binding constant of L-Pro⊂**1in** being two orders of magnitude smaller (*vide supra*). It also demonstrates that the guest exchange process is fast on the human timescale (*i.e.* min.).‡‡

Next, we studied the competitive displacement of the indicator *N*-oxide **6**, involved in the **6**⊂**1in** complex, by L-Pro and L-Pip at micromolar concentrations using emission spectroscopy. We prepared an equimolar dichloromethane solution of **6** and **1in** (1 μM). At this concentration and taking in consideration the binding constant determined in the previous section, the **6**⊂**1in** complex is present in 84% extent. Thus, the fluorescence observed for the ensemble is assigned to the 16% of dye **6** remaining free in solution (Fig. 9).

The titration of the solution with incremental amounts of L-Pro evidenced a gradual increase of the fluorescence emission. In the presence of 30 equiv. of L-Pro, the observed intensity for the maximum of the emission band was 2.5 times higher than the initial one (I_0). We rationalized the noticed fluorescence "turn-on" by considering the displacement of **6**, as quencher of the fluorescence of the phenyl-amino-naphthyl group in the **6**⊂**1in** complex, by L-Pro. This displacement leads to the formation of the fluorescent L-Pro⊂**1in** complex. It is worthy to note that the identical titration monitored using absorption spectroscopy produced negligible changes in the registered spectra.

We analysed mathematically the titration data obtained in the emission IDA experiment using a theoretical binding model considering the competitive formation of two 1 : 1 complexes (**6**⊂**1in** and L-Pro⊂**1in**). We assigned emissive properties to only two (free **1in** and L-Pro⊂**1in**) of the six species involved the binding model.§§ We fixed the binding constant of the **6**⊂**1in** complex to the previously determined value of $K = 3.2 \times 10^7$ M^{-1} (*vide supra*). The fit of the experimental data to the

‡‡The competitive displacement of guest **6** from the cavity of **1in** by L-Pro in CD_2Cl_2 was not possible at millimolar concentration due to the poor solubility of L-Pro in this solvent.

§§The **6**⊂**1in** complex was considered non-emissive under the experimental conditions and the instrument set up used for the titration (slit width of the monochromator = 1 nm).

model was good and returned the stability constant value for the L-Pro⊂**1in** as K(L-Pro⊂**1in**)$_{IDA}$ = 4.5 × 10^5 M^{-1}. This value is in good agreement with the one determined previously using direct BBS titration experiments (K(L-Pro⊂**1in**)$_{BBS}$ = 3.2 × 10^5 M^{-1}, *vide supra*). The fit of the experimental data also provided the calculated emission spectra for **1in** and L-Pro⊂**1in**. The calculation of the spectra of the emissive (*a.k.a.* coloured) species is one of the advantages of performing global fitting multivariate data analysis compared to the simpler single or even multiple wavelength fitting alternatives. Obtaining sensible calculated spectra for the coloured species is a necessary condition to support the quality and fit of the data analysis. To our delight, the calculated spectra showed a nice agreement with the experimental ones registered in separate experiments. We also tested the performance of the ensemble of **6** and **1out** in emission IDA experiments with L-Pro (Fig. S32†). Using this methodology, the calculated binding constant for the L-Pro⊂**1out** complex was K(L-Pro⊂**1out**)$_{IDA}$ = 7.9 × 10^4 M^{-1}. In short, the emission IDA experiments reflected that the difference in the binding constant values of the L-Pro⊂**1in** and L-Pro⊂**1out** inclusion complexes is close to one order of magnitude, in favour of the former. In addition, the binding constant values measured for the complexes using IDA and BBS experiments are fully consistent.

We carried out analogous IDA experiments with L-Pip. We observed a 1.7 times fluorescence enhancement for the ensemble of **6** and **1in** in the presence of 30 equiv. of L-Pip (*i.e.* I_{30} = 1.7 × I_0) (Fig. S33†). The measured fluorescence enhancement factor is reduced when compared to the 2.5-fold observed for L-Pro under identical conditions. The fit of the data of the IDA experiments to the same theoretical binding model used before for L-Pro returned a binding constant for L-Pip⊂**1in** complex of K(L-Pip⊂**1in**)$_{IDA}$ = 6.3 × 10^4 M^{-1}. Again, this value is in line with the one obtained in direct BBS experiments. It is worthy to mention that under the used experimental conditions for the IDA, and considering the calculated binding constant for the L-Pip⊂**1in** complex, this species is only formed in a 20% extent. The reduced extension in which the L-Pip⊂**1in** complex is formed diminishes the accuracy of the calculated binding constant value. Unfortunately, the low solubility of L-Pip in dichloromethane hampered the formation of the L-Pip⊂**1in** complex to a larger extent.

We also determined the binding constant of L-phenylalanine (L-Phe) with **1in** using analogous competitive IDA experiments. We observed a 1.5 times fluorescence enhancement in the presence of 30 equiv. of L-Phe (Fig. 9b). This result hinted to similar binding constant values for the L-Phe⊂**1in** and L-Pip⊂**1in** complexes. The fit of the experimental data returned a binding constant of K(L-Phe⊂**1in**)$_{IDA}$ = 3.5 × 10^4 M^{-1}.

Influence of the polar hydrogen bonding in the inclusion complexes of 1in. In previous studies, we learned that in water solution six-membered ring lactams produced more stable inclusion complexes with bis-phosphonate cavitand than the five-membered analogues.[16] These results were rationalized based on the superior size and shape fit of the 6-membered ring, with respect to the receptor's cavity, and its increased hydrophobicity. Considering our previous findings, we were surprised to calculate a larger binding constant for the L-Pro⊂**1in** complex, involving a 5-membered cyclic guest, than for the analogous complex with L-Pip (6-membered ring).

To gain some insight on the structures of the amino acid's inclusion complexes with receptor **1in**, we computed their energy-minimized structures at the BP86[17,18]/def2SVP level of theory using GAUSSIAN 09.[19] In all the computed inclusion complexes, the calix[4]pyrrole core adopts the cone conformation by establishing four hydrogen bonding interactions with one of the oxygen atoms of the carboxylate group of the included guest (Fig. 10 and Fig. S34†). It is also possible to infer the presence of multiple CH–π and O–π interactions in the complexes (Fig. S35†). Moreover, all complexes display a charged hydrogen bonding interaction between the inwardly directed P═O group of the receptor and the protonated amino group of the zwitterionic form of the bound amino acids (Fig. S35†).

In the particular case of the L-Pip⊂**1in** complex, we computed two different binding geometries. One of them involved the energetically more favourable conformation of L-Pip, L-Pip$_{eq}$ (*i.e.* COO$^-$ substituent equatorial in the protonated piperidine chair conformation). The other one considers the higher energy conformer, L-Pip$_{ax}$ (*i.e.* COO$^-$ substituent is axial in the protonated piperidine chair conformation). The results of the calculations indicated that both inclusion complexes were isoenergetic.

A simple visual inspection of the energy-minimized structures of the amino acid's inclusion complexes revealed that those of L-Pro featured a superior match in size and shape between the cavity of **1in** and the included amino acid (Fig. 10). Most likely, the L-Pro⊂**1in** inclusion complex establishes energetically more favourable dispersive, van der Waals and hydrogen bonding intermolecular interactions than the other counterparts (L-Pip⊂**1in** and L-Phe⊂**1in**) (Fig. S34†).

The experimentally determined values for the association constants of the complexes of the amino acids with receptors **1in** and **1out** are summarized in Table 1. We draw the following conclusions from the tabulated data.

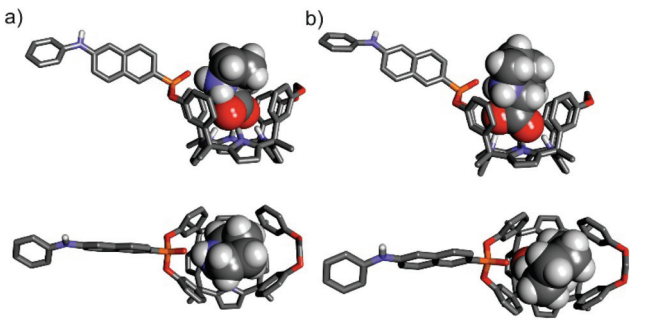

Fig. 10 Side and top views of the energy-minimized inclusion complexes L-Pro⊂**1in** (a) and L-Pip$_{eq}$⊂**1in** (b). The structures are energy minima at the BP86/def2-SVP level of theory. The receptors are shown in stick representation. Non-polar hydrogen atoms were removed for clarity. The included amino acids are depicted as CPK models.

Table 1 Binding constants K_a (M^{-1}) at 298 K for the 1 : 1 inclusion complexes of the **1in** and **1out** receptors in dichloromethane and free Gibbs energy ΔG (kcal mol^{-1})

		1in	**1out**	$\Delta\Delta G_{(\mathbf{1in}-\mathbf{1out})}$
L-Pro	K_a	$3.2 \pm 0.6 \times 10^{5a}$ $4.5 \pm 0.9 \times 10^{5b}$	$3.9 \pm 0.8 \times 10^{4a}$ $7.9 \pm 1.5 \times 10^{4b}$	~−1.1
	ΔG	-7.5 ± 0.1^{a} -7.7 ± 0.1^{b}	-6.3 ± 0.1^{a} -6.7 ± 0.1^{b}	
L-Pip	K_a	$6.3 \pm 1.3 \times 10^{4a}$ $6.3 \pm 1.3 \times 10^{4b}$	$2.3 \pm 0.5 \times 10^{4a}$	-0.5^{a}
	ΔG	-6.5 ± 0.1^{a} -6.5 ± 0.1^{b}	-6.0 ± 0.1^{a}	
L-Phe	K_a	$3.5 \pm 0.7 \times 10^{4b}$	n.d.	n.d.
	ΔG	-6.2 ± 0.1^{b}	n.d.	

K_a and ΔG are the average values from two independent titrations. Errors are reported as standard deviation for K_a and propagated for ΔG. [a] Determined by direct BBS experiments. [b] Determined by IDA experiments. n.d. Not determined.

On the one hand, the determined ΔG values for L-Pro⊂**1in** and L-Pro⊂**1out** complexes assigned a free energy gain of ~−1.1 kcal mol^{-1} ($\Delta\Delta G_{(\text{L-Pro}\subset\mathbf{1in}-\text{L-Pro}\subset\mathbf{1out})}$) in favour to L-Pro⊂**1in** complex. We attributed this difference to the additional polar hydrogen bonding interaction established in the inclusion complex with **1in**. This interaction involves the oxygen atom of the P=O group inwardly directed towards the receptor's cavity and the protonated amino group of the included L-Pro. Due to geometrical reasons, this interaction is not present in the L-Pro⊂**1out** complex. Thus, receptor **1out** binds L-Pro through the formation of only four hydrogen bonds involving the carboxylate group of the L-Pro and pyrrole NHs of **1out**. Additional CH–π interactions also assist in the stabilization of both complexes.

On the other hand, the calculated free energy difference between the analogous complexes of L-Pip ($\Delta\Delta G_{(\text{L-Pip}\subset\mathbf{1in}-\text{L-Pip}\subset\mathbf{1out})}$) is reduced to just −0.5 kcal mol^{-1}. Most likely, this is due to the formation of a weaker polar hydrogen bond in the L-Pip⊂**1in** complex in comparison to the L-Pro counterpart.

We measured a small free energy difference for the complexes of L-Pro and L-Pip with the **1out** receptor (~−6.3 and −6.0 kcal mol^{-1}, respectively) that we assigned it to the better fit of the former in the cavity of the latter. Taken together, these results indicate that the polar intermolecular hydrogen bond interaction N–H···O=P plays a pivotal role in the binding selectivity featured by **1in** for L-Pro over L-Pip, $\Delta\Delta G_{(\text{L-Pro}\subset\mathbf{1in}-\text{L-Pip}\subset\mathbf{1in})}$ ~-1.0 kcal mol^{-1}.

Conclusions

We report the synthesis of two unprecedented diastereoisomeric mono-phosphonate calix[4]pyrrole cavitands featuring a *N*-phenyl-naphthalamine fluorophore directly attached to its phosphorous atom. The two isomers differ in the relative orientation (in/out) of the P=O bridging group with respect to its polar aromatic cavity (**1in** and **1out**). We characterized the two isomers in solution using NMR and optical (UV–Vis absorption and emission) spectroscopies and in the solid state by X-ray diffraction studies. We used the non-fluorescent model receptors **5in** and **5out** to perform a competitive binding experiment with L-Pro. The analyses of the mixtures using ^{1}H and ^{31}P NMR spectroscopy showed that the L-Pro was preferentially bound to the **5in** isomer. We attributed the higher thermodynamic stability exhibited by the L-Pro⊂**5in** complex to the existence of an additional charged hydrogen bonding interaction between the protonated amino group of bound L-Pro and the inwardly directed bridging P=O function of the receptor. We developed two different supramolecular approaches for the sensing of L-Pro and L-Pip using the fluorescent receptor **1in**: direct binding-based sensing (BBS) and a FRET-based indicator displacement assay (IDA). The BBS strategy produced a small reduction of the emission intensity of **1in** upon binding L-Pro or L-Pip. The fit of the reduced emission changes to a simple 1 : 1 binding model allowed us to determine the binding constants of the inclusion complexes of **1in** with L-Pro and L-Pip as, $K(\text{L-Pro}\subset\mathbf{1in})_{BBS}$ = 3.2 × 10^5 M^{-1} and $K(\text{L-Pip}\subset\mathbf{1in})_{BBS}$ = 6.3 × 10^4 M^{-1}, respectively. Analogous titration experiments of the **1out** isomer with the two amino acids resulted in greater decreases of the emission intensity of the free receptor. In contrast, the binding constant values determined for the complexes of **1out** with L-Pro and L-Pip are close to one order of magnitude lower than those of **1in**. The increased binding affinity of the amino acids for the **1in** receptors is assigned to the charged hydrogen-bonding interaction established between the protonated amino group of the bound guest and the bridging P=O function inwardly directed with respect to the polar aromatic cavity of the receptor.

The sensing of amino acids (*e.g.* L-Pro, L-Pip and L-Phe) using IDA experiments with the ensemble composed by **1in** and *N*-oxide **6** produced more significant emission changes than those of the direct BBS strategy. Remarkably, the IDA experiments induced fluorescence "turn on" instead of quenching. The binding constant values determined for the amino acid's inclusion complexes with **1in** using IDA experiments were in complete agreement with those derived from the direct BBS counterparts. Receptor **1in** showed binding selectivity for L-Pro over the other amino acids tested. Conversely, receptor **1out** did not feature a noticeable selectivity in the amino acids' binding. We assign the dissimilar receptors' binding selectivity to the existence of an intermolecular hydrogen bond interaction between the bound amino acid and the P=O group of the receptor. For geometrical reasons, the required arrangement of functional groups is only possible for the **1in** diastereoisomer. The obtained results demonstrate the importance of dedicated polar interactions in determining binding selectivity.

Conflicts of interest

There are no conflicts to declare.

Acknowledgements

We thank Gobierno de España MCIN/AEI/FEDER, UE (projects CTQ2017-84319-P and CEX2019-000925-S), the CERCA Programme/Generalitat de Catalunya, and AGAUR (2017 SGR 1123) for financial support. We thank Dr Eduardo C. Escudero-Adán, the X-ray Diffraction Unit of ICIQ, for help with the analysis of the X-ray crystallographic data.

Notes and references

1 Z. Lou, L. Wang and G. Shen, Recent Advances in Smart Wearable Sensing Systems, *Adv. Mater. Technol.*, 2018, **3**, 1800444.
2 B. Purohit, A. Kumar, K. Mahato and P. Chandra, Smartphone-assisted personalized diagnostic devices and wearable sensors, *Curr. Opin. Biomed. Eng.*, 2020, **13**, 42–50.
3 S. Subrahmanyam, S. A. Piletsky and A. P. F. Turner, Application of Natural Receptors in Sensors and Assays, *Anal. Chem.*, 2002, **74**, 3942–3951.
4 R. Pinalli, A. Pedrini and E. Dalcanale, Biochemical sensing with macrocyclic receptors, *Chem. Soc. Rev.*, 2018, **47**, 7006–7026.
5 C. Guo, A. C. Sedgwick, T. Hirao and J. L. Sessler, Supramolecular fluorescent sensors: An historical overview and update, *Coord. Chem. Rev.*, 2021, **427**, 213560.
6 L. Pirondini and E. Dalcanale, Molecular recognition at the gas–solid interface: a powerful tool for chemical sensing, *Chem. Soc. Rev.*, 2007, **36**, 695–706.
7 M. Ciardi, F. Tancini, G. Gil-Ramírez, E. C. Escudero-Adán, C. Massera, E. Dalcanale and P. Ballester, Switching from Separated to Contact Ion-Pair Binding Modes with Diastereomeric Calix[4]pyrrole Bis-phosphonate Receptors, *J. Am. Chem. Soc.*, 2012, **134**, 13121–13132.
8 M. Ciardi, A. Galán and P. Ballester, Tetra-phosphonate Calix[4]pyrrole Cavitands as Multitopic Receptors for the Recognition of Ion Pairs, *J. Am. Chem. Soc.*, 2015, **137**, 2047–2055.
9 T. Guinovart, D. Hernandez-Alonso, L. Adriaenssens, P. Blondeau, M. Martinez-Belmonte, F. X. Rius, F. J. Andrade and P. Ballester, Recognition and Sensing of Creatinine, *Angew. Chem., Int. Ed.*, 2016, **55**, 2435–2440.
10 M. M. Erenas, I. Ortiz-Gómez, I. de Orbe-Payá, D. Hernández-Alonso, P. Ballester, P. Blondeau, F. J. Andrade, A. Salinas-Castillo and L. F. Capitán-Vallvey, Ionophore-Based Optical Sensor for Urine Creatinine Determination, *ACS Sens.*, 2019, **4**, 421–426.
11 A. F. Sierra, D. Hernández-Alonso, M. A. Romero, J. A. González-Delgado, U. Pischel and P. Ballester, Optical Supramolecular Sensing of Creatinine, *J. Am. Chem. Soc.*, 2020, **142**, 4276–4284.
12 L. Martínez-Crespo, J. L. Sun-Wang, A. F. Sierra, G. Aragay, E. Errasti-Murugarren, P. Bartoccioni, M. Palacín and P. Ballester, Facilitated Diffusion of Proline across Membranes of Liposomes and Living Cells by a Calix[4]pyrrole Cavitand, *Chem*, 2020, **6**, 3054–3070.
13 F. Maffei, P. Betti, D. Genovese, M. Montalti, L. Prodi, R. De Zorzi, S. Geremia and E. Dalcanale, Highly Selective Chemical Vapor Sensing by Molecular Recognition: Specific Detection of C1–C4 Alcohols with a Fluorescent Phosphonate Cavitand, *Angew. Chem., Int. Ed.*, 2011, **50**, 4654–4657.
14 A. C. Sedgwick, J. T. Brewster, T. Wu, X. Feng, S. D. Bull, X. Qian, J. L. Sessler, T. D. James, E. V. Anslyn and X. Sun, Indicator displacement assays (IDAs): the past, present and future, *Chem. Soc. Rev.*, 2021, **50**, 9–38.
15 B. Plecko, C. Hikel, G. C. Korenke, B. Schmitt, M. Baumgartner, F. Baumeister, C. Jakobs, E. Struys, W. Erwa and S. Stöckler-Ipsiroglu, Pipecolic Acid as a Diagnostic Marker of Pyridoxine-Dependent Epilepsy, *Neuropediatrics*, 2005, **36**, 200–205.
16 G. Peñuelas-Haro and P. Ballester, Efficient hydrogen bonding recognition in water using aryl-extended calix[4]pyrrole receptors, *Chem. Sci.*, 2019, **10**, 2413–2423.
17 J. P. Perdew, Density-functional approximation for the correlation energy of the inhomogeneous electron gas, *Phys. Rev. B: Condens. Matter Mater. Phys.*, 1986, **33**, 8822–8824.
18 A. D. Becke, Density-functional exchange-energy approximation with correct asymptotic behavior, *Phys. Rev. A*, 1988, **38**, 3098–3100.
19 M. J. Frisch, G. W. Trucks, H. B. Schlegel, G. E. Scuseria, M. A. Robb, J. R. Cheeseman, G. Scalmani, V. Barone, G. A. Petersson, H. Nakatsuji, X. Li, M. Caricato, A. Marenich, J. Bloino, B. G. Janesko, R. Gomperts, B. Mennucci, H. P. Hratchian, J. V. Ortiz, A. F. Izmaylov, J. L. Sonnenberg, D. Williams-Young, F. Ding, F. Lipparini, F. Egidi, J. Goings, B. Peng, A. Petrone, T. Henderson, D. Ranasinghe, V. G. Zakrzewski, J. Gao, N. Rega, G. Zheng, W. Liang, M. Hada, M. Ehara, K. Toyota, R. Fukuda, J. Hasegawa, M. Ishida, T. Nakajima, Y. Honda, O. Kitao, H. Nakai, T. Vreven, K. Throssell, J. A. Montgomery Jr., J. E. Peralta, F. Ogliaro, M. Bearpark, J. J. Heyd, E. Brothers, K. N. Kudin, V. N. Staroverov, T. Keith, R. Kobayashi, J. Normand, K. Raghavachari, A. Rendell, J. C. Burant, S. S. Iyengar, J. Tomasi, M. Cossi, J. M. Millam, M. Klene, C. Adamo, R. Cammi, J. W. Ochterski, R. L. Martin, K. Morokuma, O. Farkas, J. B. Foresman and D. J. Fox, *Gaussian 09, Revision A.02*, Gaussian, Inc., Wallingford, CT, 2016.

